Electronic Supplementary Material (ESI) for Organic & Biomolecular Chemistry.

SUPPORTING INFORMATION

Control of the hierarchical assembly of π-conjugated optoelectronic peptides by pH and flow

Rachael A. Mansbach[†] and Andrew L. Ferguson[*,‡,¶]

Department of Physics, University of Illinois at Urbana-Champaign, 1110 W Green St, Urbana, IL 61801, USA., and Department of Materials Science and Engineering, University of Illinois at Urbana-Champaign, 1304 W Green Street, Urbana, IL 61801, USA.

E-mail: alf@illinois.edu

Phone: (217) 300-2354. Fax: (217) 333-2736

[*]To whom correspondence should be addressed

[†]Department of Physics, University of Illinois at Urbana-Champaign, 1110 W Green St, Urbana, IL 61801, USA.

[‡]Department of Materials Science and Engineering, University of Illinois at Urbana-Champaign, 1304 W Green Street, Urbana, IL 61801, USA.

[¶]Department of Chemical and Biomolecular Engineering, University of Illinois at Urbana-Champaign, 600 South Mathews Avenue, Urbana, IL 61801, USA.

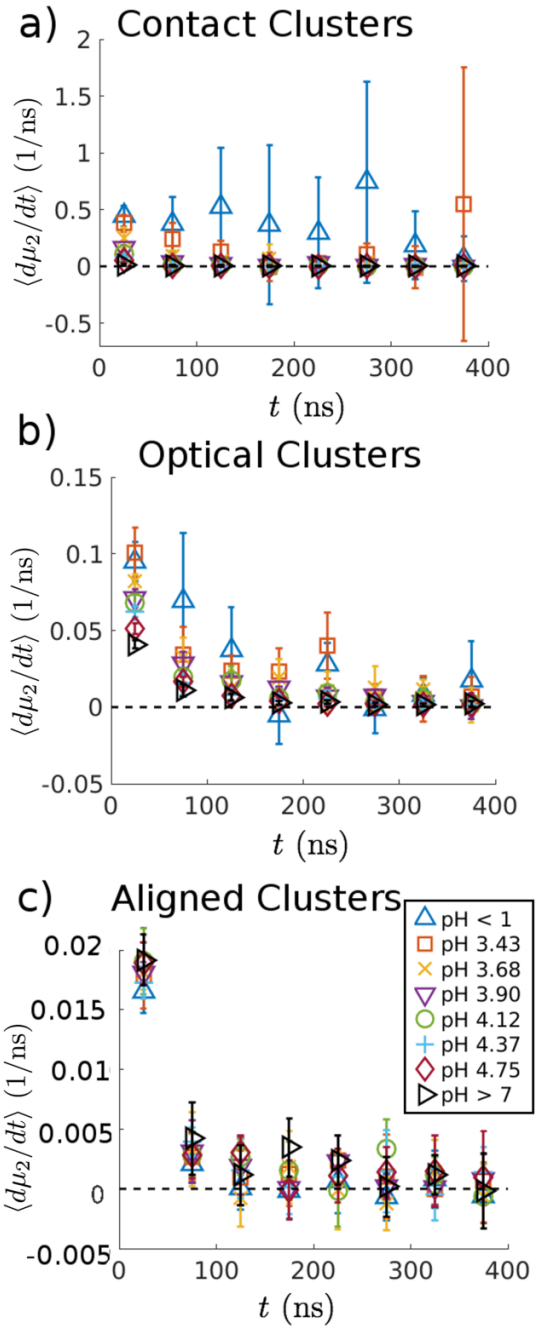

Figure S1: The time derivative of the mass-averaged cluster size $d\mu_2/dt$ in each of eight equally-sized time blocks of 50 ns over the 400 ns run at each of the eight pH values considered. Time derivatives are computed from the slope of the best linear least-squares fit over each block. Data points represent averages of the slopes over the five independent simulations at each pH, and error bars denote the corresponding standard deviations. $d\mu_2/dt$ decreases in time for all pH values, corresponding to a slowing of the growth rate. By 300 ns all slopes lie within error bars of zero, but it is not possible to conclusively state within the uncertainty of our data whether growth has been arrested or simply retarded to exceedingly low rates. This illustrates the difficulty in distinguishing between very slow growth and kinetic arrest from the time and length scales accessible to molecular simulation.

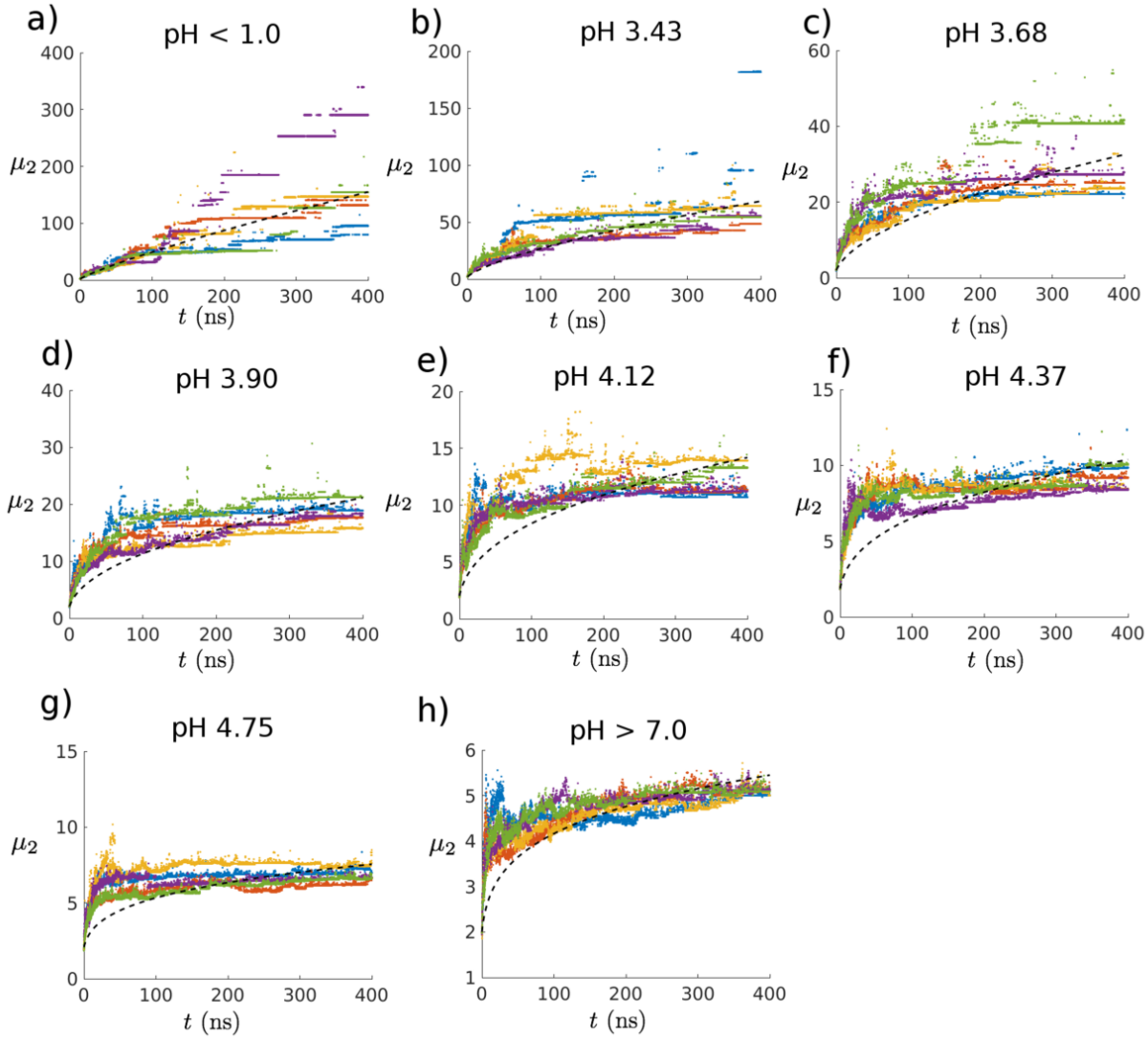

Figure S2: Mass-averaged cluster size μ_2 of contact clusters versus time at pH (a) < 1.0, (b) 3.43, (c) 3.68, (d) 3.90, (e) 4.12, (f) 4.37, (g) 4.75, and (h) > 7.0. The five independent runs conducted at each pH are denoted by different colors. The dashed lines show the Smoluchowski coagulation model predictions $\mu_2(t) = \mu_2(0)\left(1 + \frac{2t}{t_c}\right)^{\frac{1}{1-\lambda}}$ employing the optimal parameter estimates computed by finding $t_c^{\text{contact}} = (5.0198 \pm 0.0001)$ ns that minimizes the overall sum-squared error of nonlinear least-squares fitting against the simulation data of the pH-dependent λ values reported in Fig. 11.

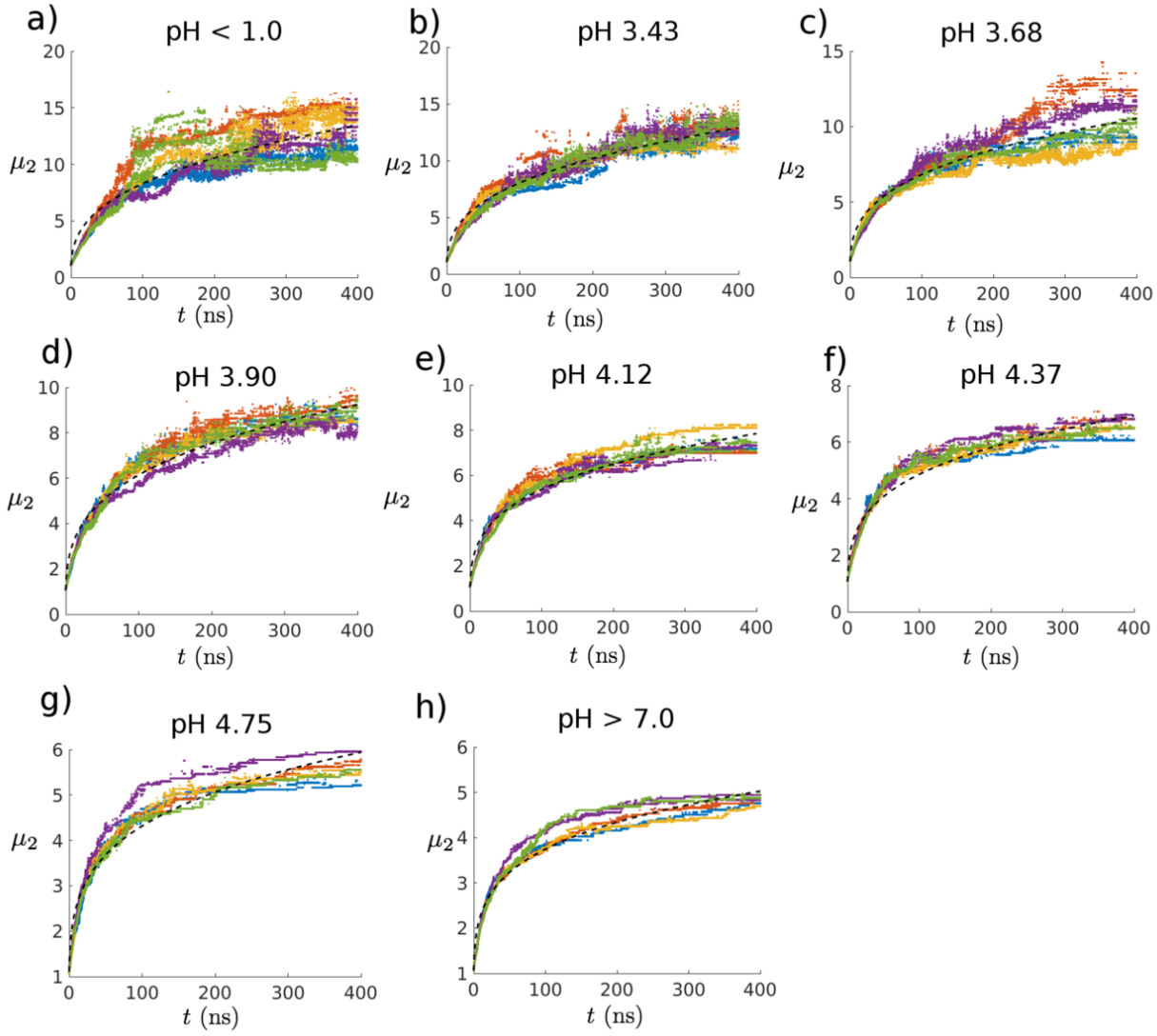

Figure S3: Mass-averaged cluster size μ_2 of optical clusters versus time at pH (a) < 1.0, (b) 3.43, (c) 3.68, (d) 3.90, (e) 4.12, (f) 4.37, (g) 4.75, and (h) > 7.0. The five independent runs conducted at each pH are denoted by different colors. The dashed lines show the Smoluchowski coagulation model predictions $\mu_2(t) = \mu_2(0)\left(1 + \frac{2t}{t_c}\right)^{\frac{1}{1-\lambda}}$ employing the optimal parameter estimates computed by finding $t_c^{\text{optical}} = (0.5564 \pm 0.0001)$ ns that minimizes the overall sum-squared error of nonlinear least-squares fitting against the simulation data of the pH-dependent λ values reported in Fig. 11.

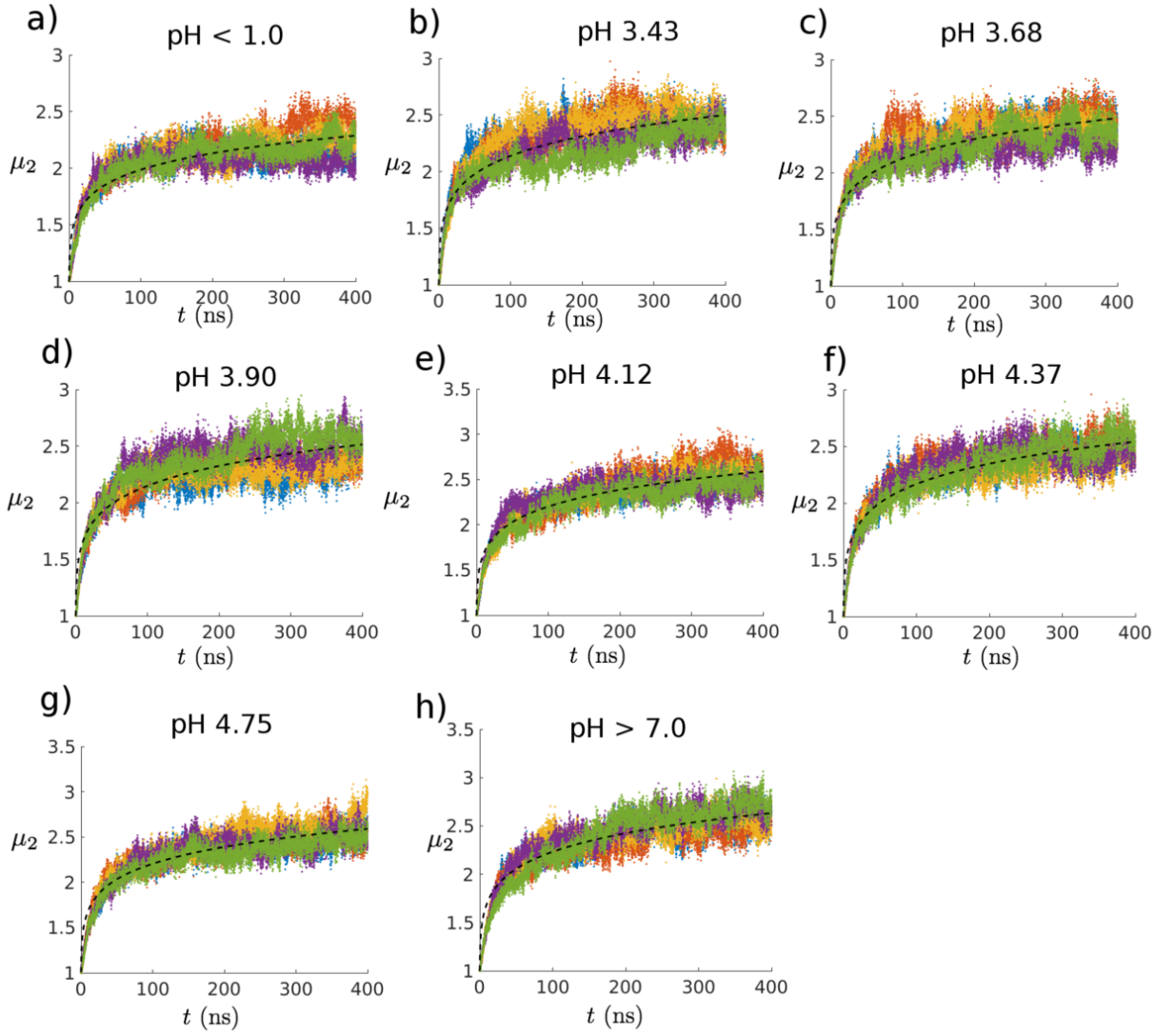

Figure S4: Mass-averaged cluster size μ_2 of aligned clusters versus time at pH (a) < 1.0, (b) 3.43, (c) 3.68, (d) 3.90, (e) 4.12, (f) 4.37, (g) 4.75, and (h) > 7.0. The five independent runs conducted at each pH are denoted by different colors. The dashed lines show the Smoluchowski coagulation model predictions $\mu_2(t) = \mu_2(0)\left(1 + \frac{2t}{t_c}\right)^{\frac{1}{1-\lambda}}$ employing the optimal parameter estimates computed by finding $t_c^{\text{aligned}} = (0.2377 \pm 0.0001)$ ns that minimizes the overall sum-squared error of nonlinear least-squares fitting against the simulation data of the pH-dependent λ values reported in Fig. 11.

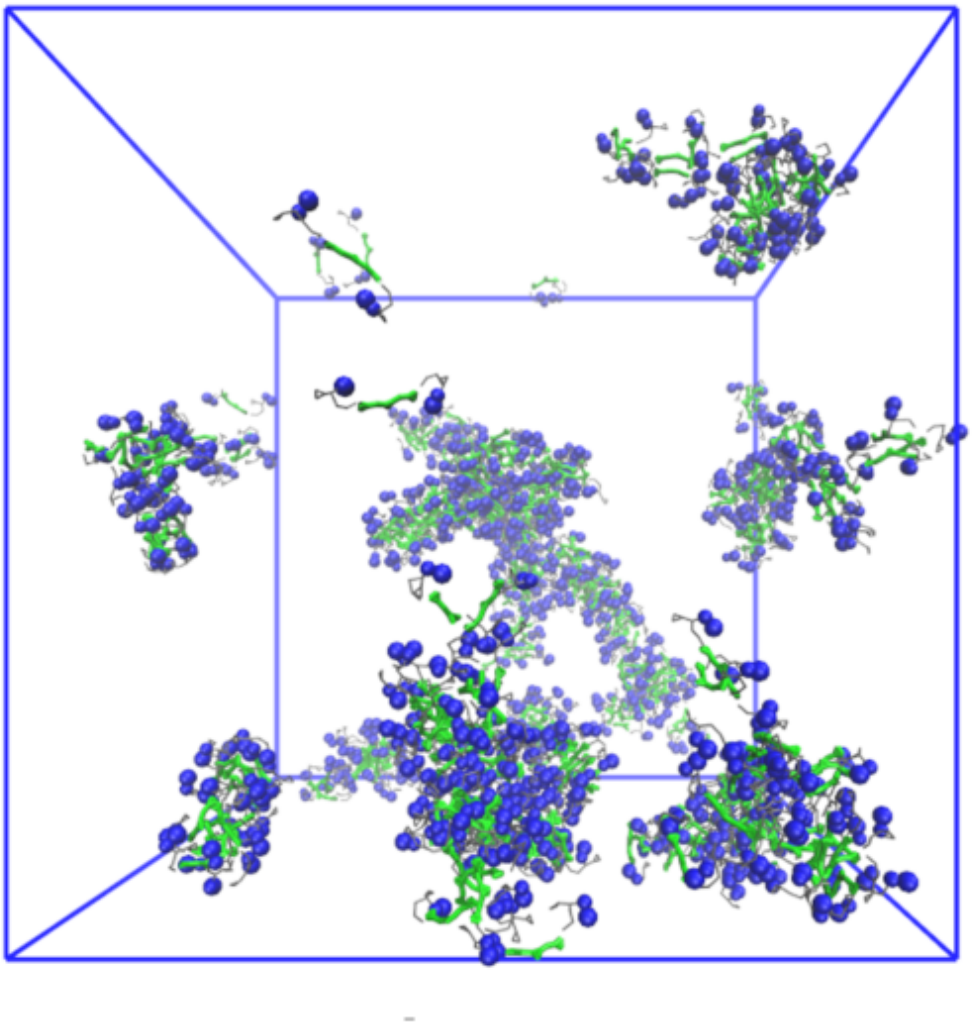

Movie M1: Simulation at 0% charge, corresponding to pH < 1, from which the snapshot in Fig. 9a in the Main Text was drawn. Aromatic cores are rendered as green bonds, side chains as grey lines, charged termini as red beads, and uncharged termini as blue beads. Coarse-grained water is omitted for clarity. The simulation trajectory is 400 ns with frames rendered every 2.5 ns.

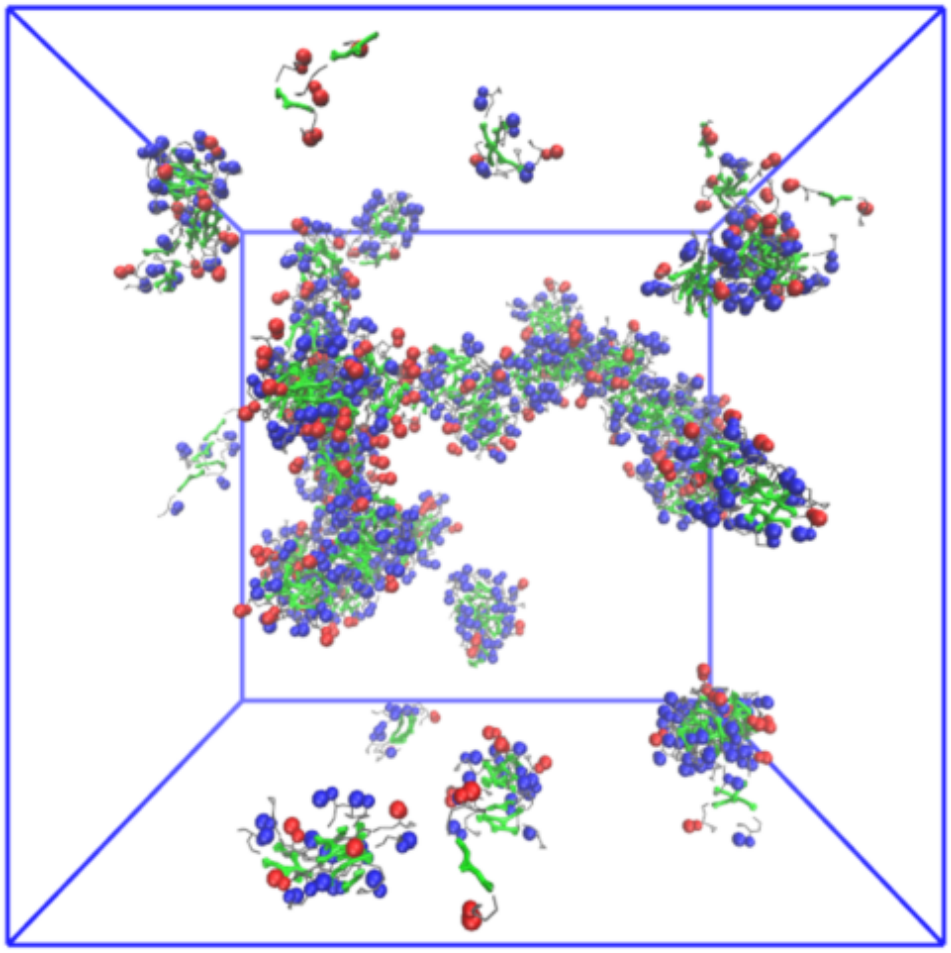

Movie M2: Simulation at 25.13% charge, corresponding to pH 3.43, from which the snapshot in Fig. 9b in the Main Text was drawn. Aromatic cores are rendered as green bonds, side chains as grey lines, charged termini as red beads, and uncharged termini as blue beads. Coarse-grained water is omitted for clarity. The simulation trajectory is 400 ns with frames rendered every 2.5 ns.

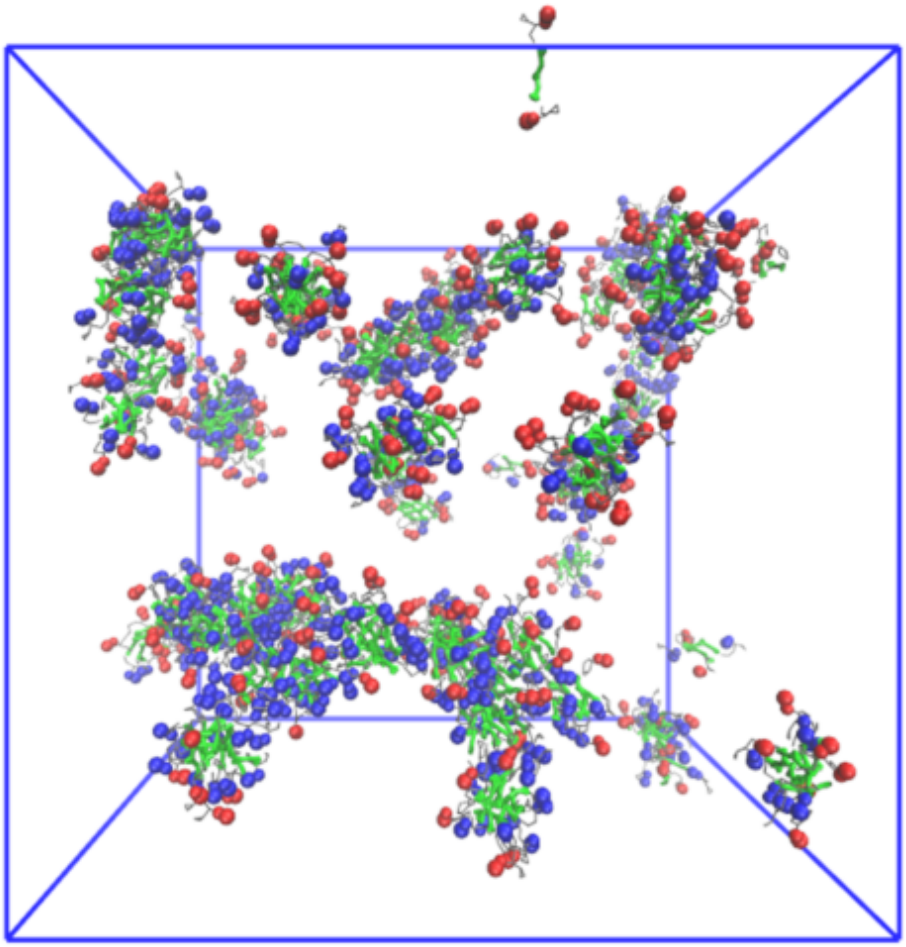

Movie M3: Simulation at 37.57% charge, corresponding to pH 3.68, from which the snapshot in Fig. 9c in the Main Text was drawn. Aromatic cores are rendered as green bonds, side chains as grey lines, charged termini as red beads, and uncharged termini as blue beads. Coarse-grained water is omitted for clarity. The simulation trajectory is 400 ns with frames rendered every 2.5 ns.

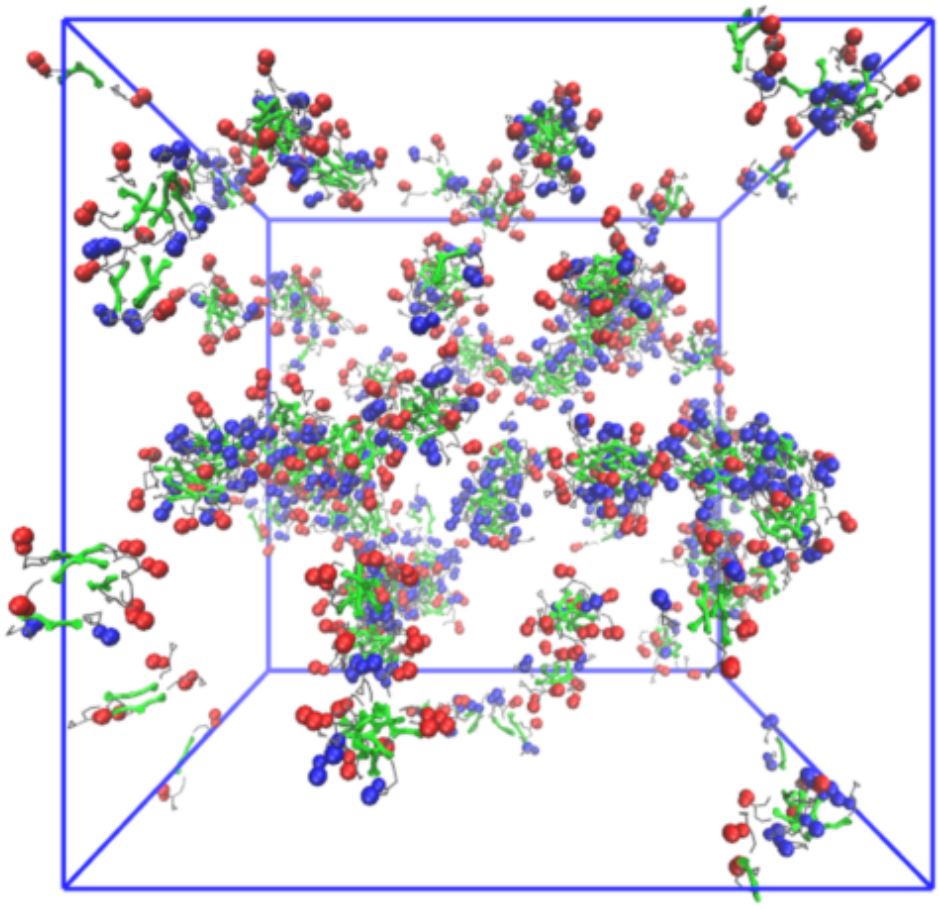

Movie M4: Simulation at 50.00% charge, corresponding to pH 3.90, from which the snapshot in Fig. 9d in the Main Text was drawn. Aromatic cores are rendered as green bonds, side chains as grey lines, charged termini as red beads, and uncharged termini as blue beads. Coarse-grained water is omitted for clarity. The simulation trajectory is 400 ns with frames rendered every 2.5 ns.

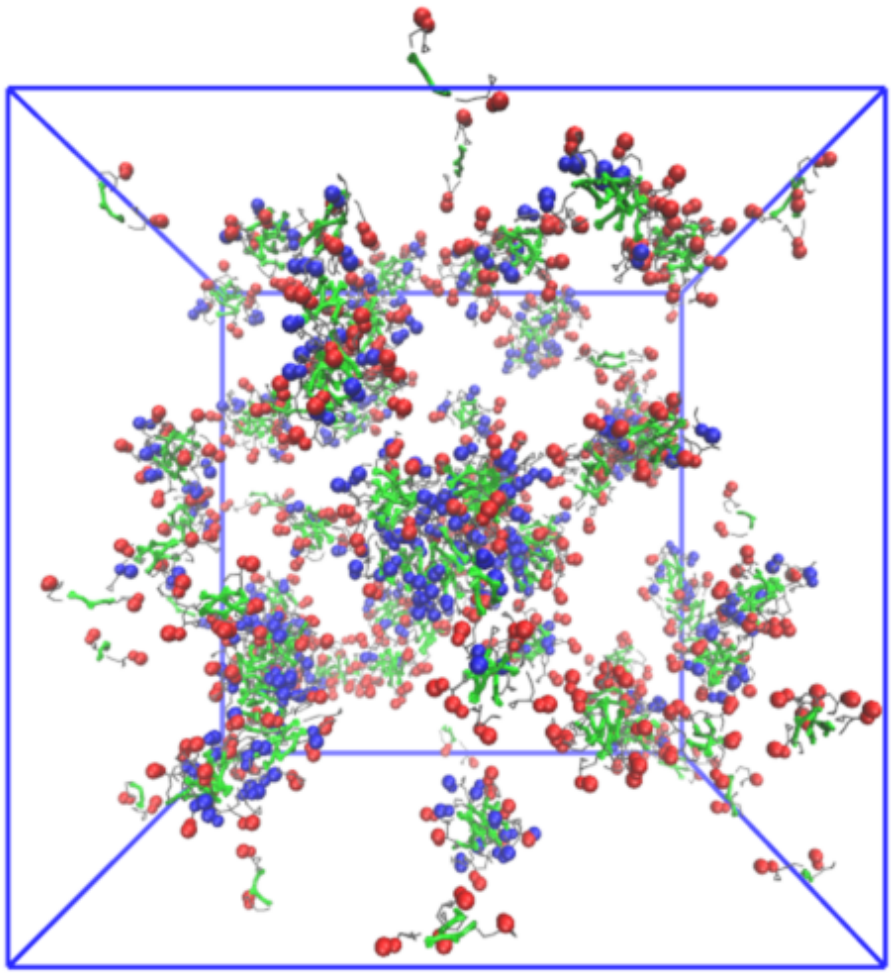

Movie M5: Simulation at 62.43% charge, corresponding to pH 4.12, from which the snapshot in Fig. 9e in the Main Text was drawn. Aromatic cores are rendered as green bonds, side chains as grey lines, charged termini as red beads, and uncharged termini as blue beads. Coarse-grained water is omitted for clarity. The simulation trajectory is 400 ns with frames rendered every 2.5 ns.

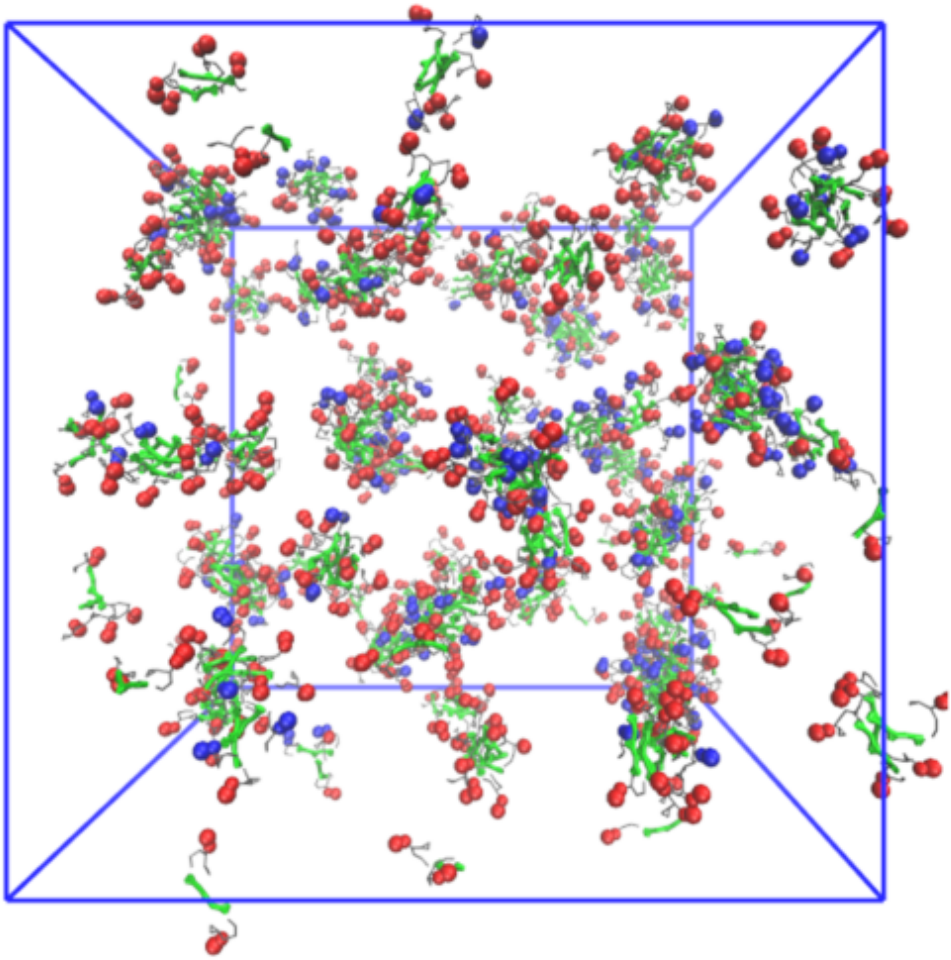

Movie M6: Simulation at 74.87% charge, corresponding to pH 4.37, from which the snapshot in Fig. 9f in the Main Text was drawn. Aromatic cores are rendered as green bonds, side chains as grey lines, charged termini as red beads, and uncharged termini as blue beads. Coarse-grained water is omitted for clarity. The simulation trajectory is 400 ns with frames rendered every 2.5 ns.

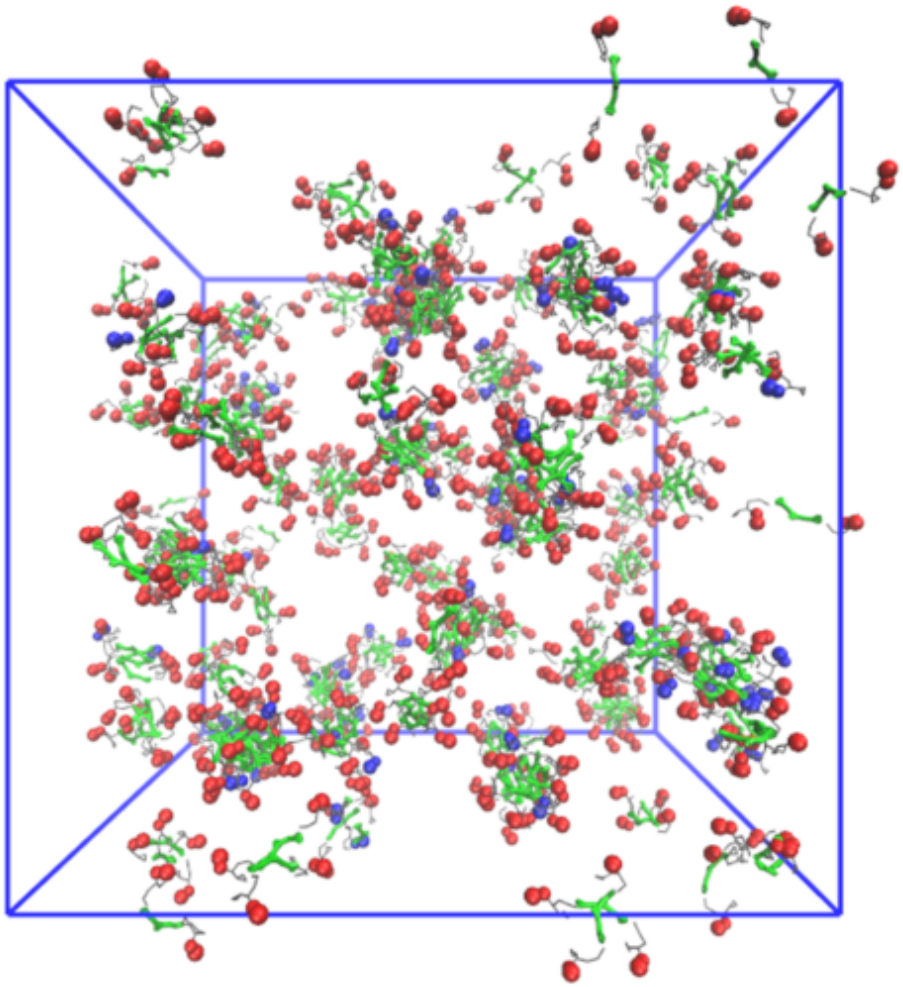

Movie M7: Simulation at 87.57% charge, corresponding to pH 4.75, from which the snapshot in Fig. 9g in the Main Text was drawn. Aromatic cores are rendered as green bonds, side chains as grey lines, charged termini as red beads, and uncharged termini as blue beads. Coarse-grained water is omitted for clarity. The simulation trajectory is 400 ns with frames rendered every 2.5 ns.

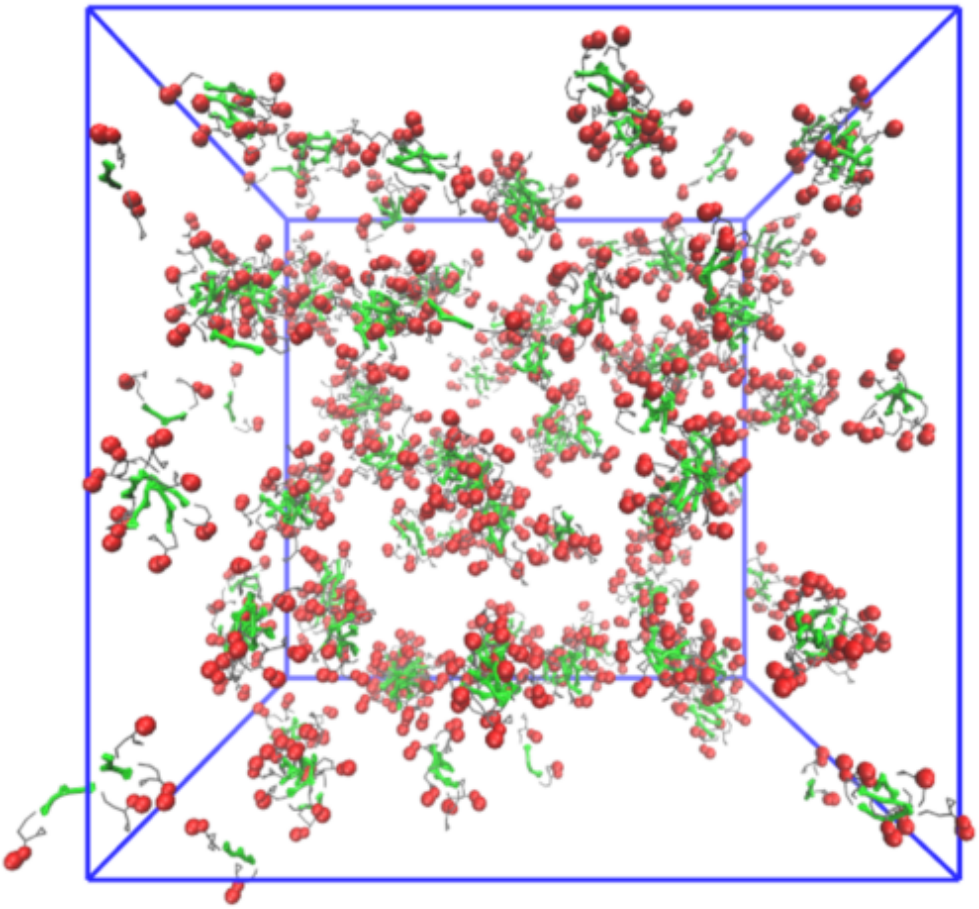

Movie M8: Simulation at 100% charge, corresponding to pH > 7, from which the snapshot in Fig. 9h in the Main Text was drawn. Aromatic cores are rendered as green bonds, side chains as grey lines, charged termini as red beads, and uncharged termini as blue beads. Coarse-grained water is omitted for clarity. The simulation trajectory is 400 ns with frames rendered every 2.5 ns.